Using Fisher information to quantify uncertainty in environmental parameters estimated from correlated ambient noise

Shane C. Walker,[a] Caglar Yardim, and Aaron Thode
Marine Physical Laboratory, Scripps Institution of Oceanography, La Jolla, California 92093-0238
scwalker@ucsd.edu, cyardim@ucsd.edu, athode@ucsd.edu

Ery Arias-Castro
Department of Mathematics, University of California San Diego, La Jolla, California 92037
eariasca@ucsd.edu

Abstract: Efforts to characterize environmental parameters from ambient noise must contend with uncertainty introduced by stochastic fluctuations of the noise itself. This Letter calculates the Fisher information and Cramer-Rao bound of an unbiased correlated ambient noise parameter estimate. As an illustration, lower bounds on the error covariance of medium speed and attenuation parameters are obtained for a two-dimensional isotropic ambient noise scenario. The results demonstrate that an optimal sensor separation exists for obtaining the minimum error and the predictions are validated using simulated parameter inversions. The influences of record length, bandwidth, signal-to-noise, and spatial resolution are discussed.

PACS numbers: 43.60.Cg, 43.30.Pc, 43.60.Pt, 43.30.Re [GD]
Date Received: November 13, 2012 **Date Accepted:** February 5, 2013

1. Introduction

In 1953 Eckart[1] demonstrated that the second order statistics of diffuse noise can exhibit spatio-temporal correlations related to the propagation of waves between two locations. In recent years, passive applications in ocean acoustics[2] and seismics[3] have capitalized on this connection to infer information about the propagation environment (e.g., phase speed, attenuation, boundary properties, etc.). Such strategies must contend with uncertainty introduced by stochastic fluctuations of the noise itself. The level of uncertainty depends on many factors including the parameters of interest, the inversion strategy, the propagation medium, the directivity of the noise, sensor geometry, sample duration (record length), and bandwidth.

A number of theoretical studies address parameter inversion uncertainty in the context of active tomography and passive source localization where the emphasis is on the information about a localized radiator (a transduction device, a ship, an earthquake, etc.) against interference from a background of diffuse ambient noise.[4,5] Here attention is paid to the passive tomography context where the focus is on environmental information carried by correlated diffuse ambient noise. Starting with a parametric model for the ambient noise covariance between a pair of spatially separated sensors, a general expression for the Fisher information (FI) with respect to chosen parameters of the model is derived and used to quantify the Cramer-Rao bound (CRB) on the estimation error. As an illustration, the FI is calculated with respect to medium phase speed and attenuation for the canonical model of isotropic broadband noise in a two-dimensional (2D), free space, attenuating medium.[6] From this follow expressions

[a]Author to whom correspondence should be addressed.

for the error bound that depend explicitly on record length, bandwidth, and sensor separation. As a consequence of the trade-off between increased signal-to-noise at small separation versus increased resolution at large separation, the error bounds exhibit a global minimum at an optimal, intermediate value of separation.

Expressions are derived for two different inversion strategies: one based on an association between peak covariance and travel-time between the sensors,[7,8] and one that incorporates the full structure of the covariance. Favorable comparison with parameter inversions carried out using simulated data suggest the FI may be useful for the design, analysis, and interpretation of ambient noise inversion experiments.

2. The Fisher information

Consider the sample covariance, $C(t,\,\tau)=x_1(t)x_2(t+\tau)$, between experimental measurements x_1 at location $\boldsymbol{r}_1$ at time t and x_2 at location $\boldsymbol{r}_2$ at time $t+\tau$. Relative time τ is referred to henceforth as lag. For simplicity, measurements x_1 and x_2 are assumed to be real valued, zero mean, Gaussian distributed, wide-sense stationary processes. As a particular realization of a stochastic process, the sample covariance exhibits fluctuations. An underlying assumption of experimental efforts to estimate a set of environmental parameters, $\boldsymbol{\theta} \equiv [\theta_1,\,\theta_2,\,\ldots,\theta_J]$, from ambient noise is that the measurement ensemble stochastically converges[9] to an expectation value, $\mathrm{C} \equiv \mathrm{C}(\tau,\,\boldsymbol{\theta})=\langle C(t,\,\tau)\rangle$, that can be modeled in terms of $\boldsymbol{\theta}$.

In the parlance of estimation theory, the stochastic fluctuations of observable $C(t,\,\tau)$ translate to error (or uncertainty) on $\boldsymbol{\theta}$. This section calculates the Fisher information matrix (FIM) for the process from which lower bounds on the error follow. In the following, vector and matrix quantities are noted in bold, with matrices having the additional underline notation. The notation $\mathbf{T}$ denotes matrix transpose.

Let $\boldsymbol{X} \equiv [x_1(t),\,x_2(t+\tau)]^{\mathrm{T}}$ represent the joint measurement of a single sample of x_1 at time t and x_2 at time $t+\tau$. The likelihood function, denoted $\mathcal{L} \equiv \mathcal{L}(\boldsymbol{\theta}|\boldsymbol{X})$, is given by $\mathcal{L}=(2\pi\ |\underline{\boldsymbol{\Sigma}}|^{1/2})^{-1}\exp(-(1/2)\boldsymbol{X}^{\mathrm{T}}\underline{\boldsymbol{\Sigma}}^{-1}\boldsymbol{X})$, where $\underline{\boldsymbol{\Sigma}} \equiv \begin{bmatrix}\sigma_1^2 & \mathrm{C}\\ \mathrm{C} & \sigma_2^2\end{bmatrix} \equiv \nu\begin{bmatrix}\xi & \rho\\ \rho & \xi^{-1}\end{bmatrix}$ is the covariance matrix, σ_1^2 (σ_2^2) is the variance of x_1 (x_2), and the definitions $\nu \equiv \sigma_1\sigma_2$, $\xi \equiv \sigma_1/\sigma_2$, and $\rho \equiv \mathrm{C}/\nu$ are used. The latter is recognized as the correlation coefficient.[10] In general, ρ, ν, and ξ can depend on $\boldsymbol{\theta}$. For a single time sample, element j,j' of the FIM with respect to two scalar parameters $\theta_j,\theta_{j'}$, given by[10] $\mathcal{I}_{jj'} \equiv [\underline{\boldsymbol{\mathcal{I}}}]_{jj'} = (1/2)\mathrm{Tr}\{\underline{\boldsymbol{\Sigma}}^{-1}\underline{\dot{\boldsymbol{\Sigma}}}_j\underline{\boldsymbol{\Sigma}}^{-1}\underline{\dot{\boldsymbol{\Sigma}}}_{j'}\}$, becomes

$$\mathcal{I}_{jj'} = \dot{\nu}_j\dot{\nu}_{j'}/\nu^2 + \frac{\nu\ddot{\xi}_j\ddot{\xi}_{j'} - \xi^2\rho(\dot{\nu}_j\dot{\rho}_{j'} + \dot{\nu}_{j'}\dot{\rho}_j)}{\nu\xi^2(1-\rho^2)} + \dot{\rho}_j\dot{\rho}_{j'}(1+\rho^2)/(1-\rho^2)^2, \tag{1}$$

where the notation $\dot{b}_j \equiv \partial b/\partial\theta_j$ denotes partial differentiation of quantity b with respect to θ_j, and $\mathrm{Tr}\{\,\}$ denotes the matrix trace.

Because the FI is additive under independence,[11] the FIM for $\mathbf{N}$ independent samples, $[\boldsymbol{X}(t_1,\tau),\boldsymbol{X}(t_2,\tau),\ldots,\boldsymbol{X}(t_{\mathrm{N}},\tau)]^{\mathrm{T}}$, is given by $\underline{\boldsymbol{I}}(\tau)=\sum_{n=1}^{\mathrm{N}}\underline{\boldsymbol{\mathcal{I}}}(\tau) = \mathrm{N}\underline{\boldsymbol{\mathcal{I}}}(\tau)$. For a measurement accumulated over a continuous collection of samples spanning duration T, the number of independent samples (on average) is given by $\mathrm{N}=T/\mathrm{t}_c$, where t_c denotes a correlation time. Consider the case (discussed in Sec. 3 below) where measurements x_1 and x_2 are white noise processes band-pass filtered over the interval $f_0(1-\Delta/2) \le |f| \le f_0(1+\Delta/2)$ about a chosen characteristic (i.e., carrier) frequency f_0. By definition, Δ must be less than 2, with $\Delta=1$ corresponding to 100% relative bandwidth. In this case, measurements sampled over interval $\mathrm{t}_c=\mathcal{F}^{-1}$ (where $\mathcal{F} \equiv 2\Delta f_0$ denotes the bandwidth) are completely uncorrelated,[12] yielding $\mathrm{N}=T\mathcal{F}$ independent samples.[13]

By similar logic the FIM for a simultaneous joint measurement over K independent values of lag, $[\boldsymbol{X}(t,\,\tau_1),\,\boldsymbol{X}(t,\,\tau_2),\ldots,\,\boldsymbol{X}(t,\,\tau_{\mathrm{K}})]^{\mathrm{T}}$, becomes $\underline{\boldsymbol{I}} = \sum_{k=1}^{\mathrm{K}}\underline{\boldsymbol{\mathcal{I}}}(\tau_k)$. In the continuous lag limit, the FIM for a duration T measurement integrated over lag becomes $\underline{\mathbf{I}} = \mathrm{t}_c^{-1}\int_{-\infty}^{\infty}d\tau\,\underline{\boldsymbol{I}}(\tau) = \mathrm{N}\mathcal{F}\int_{-\infty}^{\infty}d\tau\underline{\boldsymbol{\mathcal{I}}}(\tau)$.

3. Demonstration: 2D isotropic ambient noise

As a demonstration, the FI and error bounds with respect to medium speed and attenuation are derived and analyzed for an ambient noise scenario involving a uniform spatial distribution of noise sources in a 2D free space attenuating medium. As the scenario is spatially homogeneous, signals x_1 and x_2 exhibit equal variance, $\sigma_1 = \sigma_2 = \sigma$ ($\xi = 1$; $\dot{\xi}_j = \dot{\xi}_{j'} = 0$). For simplicity the analysis assumes x_1 and x_2 exhibit white power spectra whose intensity is independent of the parameters of interest[14] ($\nu = \sigma^2$; $\dot{\nu}_j = \dot{\nu}_{j'} = 0$).

By the correlation theorem, the correlation coefficient is given by

$$\rho(\tau) = \frac{\mathrm{C}(\tau)}{\nu} = \frac{2}{\mathcal{F}} \mathcal{R}e\left\{ \int_{f-}^{f+} df\, \Gamma \exp(i2\pi f \tau) \right\}, \tag{2}$$

where $\Gamma \equiv \Gamma(f)$ denotes the coherence function between x_1 and x_2 with respect to frequency and the limits of integration are defined $f_\pm \equiv f_0(1 \pm \Delta/2)$. The factor of $\mathcal{F}^{-1}$ is required for consistency with the condition $\xi = 1$. For the isotropic 2D scenario of interest, the coherence function takes the form[6] $\Gamma = \exp(-ad) J_0(2\pi df/c)$, where J_0 denotes the zeroth order Bessel function of the first kind, $d = |\boldsymbol{r}_1 - \boldsymbol{r}_2|$ is the sensor separation, and c and a are the medium speed and attenuation, respectively.

To avoid mixed dimensionality, dimensionless parameters are introduced: $\boldsymbol{\theta} \equiv [\mathrm{c}, \mathrm{a}]$, where $\mathrm{c} \equiv c/c_0$ and $\mathrm{a} \equiv a/a_0$ represent the speed and attenuation, respectively, referenced to particular values $c = c_0$ and $a = a_0$. At the characteristic frequency, f_0, one can then define $\lambda_0 \equiv c_0/f_0$, $\mu \equiv d/\lambda_0$, and $\alpha \equiv a_0\lambda_0$ as the characteristic wavelength, the sensor aperture in wavelengths, and the attenuation coefficient in nepers per wavelength, respectively. While an analytic solution in terms of elementary functions is not possible, using the asymptotic form, $\Gamma \sim \pi^{-1}\sqrt{(f_0\mathrm{c})/(f\mu)}\cos(2\pi\mu f/f_0\mathrm{c} - \pi/4) \times \exp(-\mathrm{a}\alpha\mu)$, to evaluate Eq. (2) at lag $\tau_d \equiv d/c$ (where the covariance exhibits a peak) in the large aperture limit, $\mu \gg 1$, yields $\rho_p \equiv \rho(\tau_d) \sim \exp(-\mathrm{a}\alpha\mu)\sqrt{\mathrm{c}}/(2\pi\sqrt{2\mu})$. Under these conditions the parametric derivatives for speed and attenuation become $\dot{\rho}_{\mathbf{c}} \equiv \dot{\rho}_{\mathbf{c}}(\tau_d) \sim -(2\pi\mu/\mathrm{c}^2)\rho_p$ and $\dot{\rho}_{\mathrm{a}} \equiv \dot{\rho}_{\mathrm{a}}(\tau_d) \sim -\alpha\mu\rho_p$, respectively. In subsequent discussion, notation $\sim$ implies the asymptotic limit assumption, $\mu \gg 1$.

3.1 Fisher information with respect to speed and attenuation

Applying Eq. (1) to the isotropic scenario defined above, the FIM associated with the covariance peak, $\underline{\boldsymbol{\mathcal{I}}}_p \equiv \underline{\boldsymbol{\mathcal{I}}}(\tau_d)$, is written

$$\underline{\boldsymbol{\mathcal{I}}}_p = \begin{bmatrix} \dot{\rho}_{\mathrm{c}}^2 & \dot{\rho}_{\mathrm{c}}\dot{\rho}_{\mathrm{a}} \\ \dot{\rho}_{\mathrm{c}}\dot{\rho}_{\mathrm{a}} & \dot{\rho}_{\mathrm{a}}^2 \end{bmatrix} \frac{1+\rho_p^2}{(1-\rho_p^2)^2} \sim (\mu\rho_p)^2 \begin{bmatrix} (2\pi/\mathrm{c}^2)^2 & 2\pi\alpha/\mathrm{c}^2 \\ 2\pi\alpha/\mathrm{c}^2 & \alpha^2 \end{bmatrix}. \tag{3}$$

As demonstrated in Fig. 1, the asymptotic expression of Eq. (3) provides a suitable approximation to the numerical result calculated using Eq. (2). From Sec. 2, the FIM for a duration T measurement is simply $\underline{\boldsymbol{I}}_p \equiv \mathrm{N}\underline{\boldsymbol{\mathcal{I}}}_p$.

Equation (3) exhibits a maximum at an aperture value $\mu_{\max} = (2\alpha)^{-1}$. In interpreting this result, it is instructive to express the FIM in terms of a signal-to-noise metric (SNR). A common approach to formulating SNR for ambient noise applications[3] is to compare the expectation of the amplitude of the peak covariance to the expectation of the sample fluctuation magnitude. Using ν_{N} to denote the expectation of the magnitude of the fluctuations of the covariance for a measurement comprising N independent samples,[15] the expectation of the SNR becomes $\mathcal{Q} \equiv \mathrm{C}(\tau_d)/\nu_{\mathrm{N}} \sim \rho_p\sqrt{\mathrm{N}} \propto (\mathrm{N}/\mu)^{1/2}\exp(-\mathrm{a}\alpha\mu)$. Recasting $\underline{\boldsymbol{I}}_p$ in terms of SNR, $\underline{\boldsymbol{I}}_p \propto (\mu\mathcal{Q})$,[2] the dependence of the FI on sensor separation can be interpreted as a tradeoff between resolution and SNR. Though the SNR may be high for small values of sensor separation, the aperture, μ, is small, resulting in poor resolution and low FI (which implies high error).

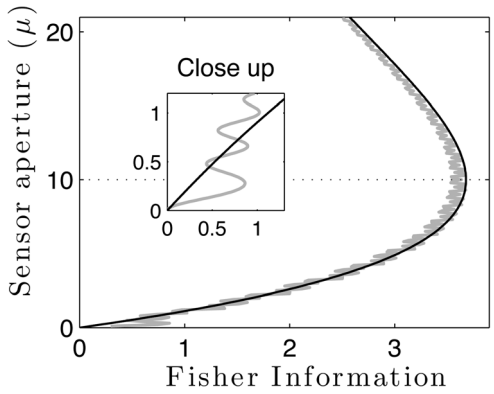

Fig. 1. The FI (horizontal) with respect to speed as a function of sensor aperture (vertical). The asymptotic form of $[\underline{\boldsymbol{I}}_{p11}]$ (black curve) is compared to the numerically evaluated exact result (gray curve). The speed and attenuation parameters are taken as unity ($c = a = 1$) with $\alpha = 0.05$. The FI is maximal at $\mu = \mu_{max} = (2\alpha)^{-1} = 10$ (dotted line) and vanishes in the limit $\mu \to 0$ (close up).

As aperture increases, improved directional discrimination tends to compensate for decreasing SNR, resulting in an optimal sensor separation, $d = \lambda_0 \mu_{max}$, for estimating the speed and attenuation. The optimal separation distance increases with decreasing attenuation. In a nonattenuating medium ($\alpha \to 0$) the value of μ_{max} diverges so that the FI increases monotonically with sensor separation.

3.2 Estimation error for speed and attenuation parameters

In the context of parameter estimation applications, the practical importance of the FI derives from its relationship with the CRB, $\underline{\mathbf{V}} = \underline{\boldsymbol{I}}^{-1}$, which sets a theoretical lower limit on the observed parameter error covariance for an unbiased estimator.[10] Depending on the estimator, the observed error may or may not approach the theoretical limit set by the CRB. When it does, the estimator is said to be efficient. In this case, the bound can be treated as a predictive quantity. For the FI approach to be most useful, it would be advantageous if it led to predictive bounds. To demonstrate that it does, this section uses Eq. (3) to derive bounds for two different estimators of speed and attenuation and compares them to the results of a parameter estimation carried out on simulated data. The following definitions are used in the subsequent discussion:

$$I_c \equiv [\underline{\boldsymbol{I}}_p]_{11} \sim N(2\pi\rho_p\mu/c^2)^2 \quad \text{and} \quad I_a \equiv [\underline{\boldsymbol{I}}_p]_{22} \sim N(\rho_p\mu\alpha)^2. \tag{4}$$

For clarity, henceforth the notation $\widetilde{b}$ is used to distinguish observed (or measured) quantities from theoretical ones.

3.2.1 Fisher information for a covariance peak/travel-time estimator

Consider a duration T measurement of the sample covariance as a function of lag, $\widetilde{C}_T(\tau) \equiv T^{-1}\int_0^T dt\, \tilde{x}_1(t)\tilde{x}_2(t+\tau)$. A simple strategy (referred to here as the peak estimator, PE) for estimating the medium speed from broadband isotropic noise in a nondispersive medium is to associate the lag at which the observed covariance exhibits a peak (see $\widetilde{\tau}$ in Fig. 2) with a travel-time, $\tau_d \equiv d/c$, between the sensors.[7,8] In formulating the FI, it is important to recognize that the finite width of the peak introduces an inherent temporal ambiguity to the estimate of τ_d. Consequently, the factor ρ_p in Eq. (4) should be replaced with $\rho_p \to (t_p/t_c) \times \rho_p = (\Delta/2)\rho_p$, where the $t_p \equiv (4f_0)^{-1}$ represents the half maximum width of the peak. Using this, the FI with respect to speed becomes $I_c^{PE} \sim (\Delta^2/4)I_c$. As the observed peak magnitude (see $\widetilde{C}_p$ in Fig. 2) is unaffected by the peak width, the appropriate FI for attenuation is simply $I_a^{PE} \sim I_a$.

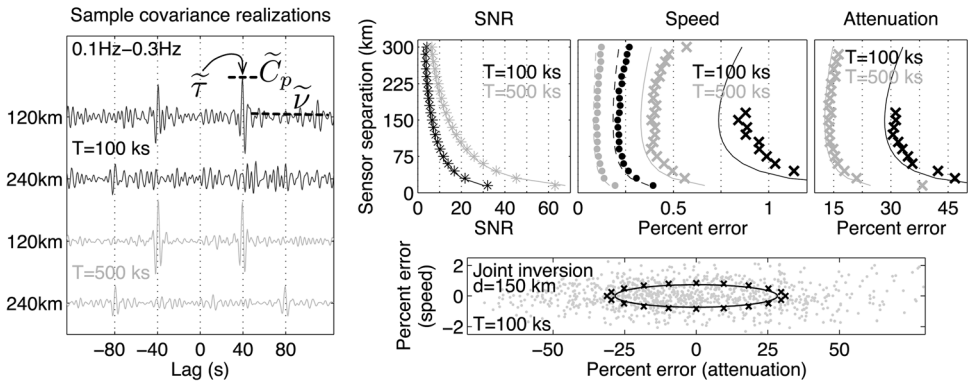

Fig. 2. Comparison of observed and predicted inversion error. A selection of realizations of the sample covariance for duration $T = 100$ ks (gray) and $T = 500$ ks (black) measurements at sensor separations, $d = 120$ km and $d = 240$ km (left panel) includes schematic examples of $\widetilde{C}_p$, $\tilde{\tau}$, and $\tilde{\nu}$. The ensemble average of the observed SNR, $\widetilde{Q}(*)$, is compared to its expectation, $\mathcal{Q}$ (solid curves). The observed ensemble average of the errors, $\tilde{\delta}$, for the PE ($\times$) and FE ($\bullet$) speed estimates are compared to the PE (dashed) and FE (solid) CRB. A similar comparison between the observed PE result ($\times$) and corresponding bound (dashed) is presented for the attenuation parameter (FE attenuation estimate omitted to facilitate viewing). Finally, the ensemble of PE estimates (gray dots) appears along with the corresponding observed error ellipse ($\times$) and the bound (black curve).

3.2.2 Fisher information for a full covariance estimator

As a more sophisticated estimation strategy (referred to here as the full-signal estimator, FE), consider an objective function, $\Phi \equiv \int_{-\infty}^{\infty} d\tau (\widetilde{C}_T(\tau) - \mathrm{C}(\tau))^2$, that utilizes the information at all values of lag, not just the lag of the peak.[16] To account for the added information of this estimator, it is appropriate to define an FI that is accumulated over all values of lag. Applying Parseval's theorem in conjunction with the additivity property discussed in Sec. 2, the appropriate FI for speed becomes $\mathrm{I}_{\mathrm{c}}^{\mathrm{FE}} \equiv \mathrm{N}\mathcal{F}\int_{-\infty}^{\infty} d\tau [\underline{\mathcal{I}}(\tau)]_{11} \sim (2\mathrm{N}/\mathcal{F})\int_{f_-}^{f^+} df |\dot{\Gamma}_{\mathrm{c}}|^2 \sim 4I_{\mathrm{c}}$, where the asymptotic form for the parametric derivative of the noise coherence model, $\dot{\Gamma}_{\mathrm{c}} \sim -\sqrt{4\mu f/f_0 \mathrm{c}^3} \times \cos((2\pi\mu f/f_0 \mathrm{c}) - (3\pi/4))\exp(-\mathrm{a}\alpha\mu)$, has been used [see discussion of Eq. (2)].

3.2.3 Comparison with parameter inversion

To demonstrate that the calculated bounds are indeed predictive they are compared to the results of a set of inversions for speed and attenuation carried out on simulated data generated using a standard matrix decomposition approach.[17] The data ensemble comprises $\mathrm{M} = 1000$ realizations of duration T samples of $\tilde{x}_1(t)$ and $\tilde{x}_2(t)$. As the 2D scenario considered has relevance for efforts in seismics[7,18] to characterize Rayleigh surface waves (which are essentially 2D, though they do exhibit dispersion), it is interesting to frame the analysis in the context of seismic ambient noise in the microseism regime: characteristic frequency $f_0 = 0.2$ Hz, relative bandwidth $\Delta = 1 (f_- = 0.1$ Hz, $f_+ = 0.3$ Hz), medium phase speed $c_0 = 3.0$ km/s (characteristic wavelength $\lambda_0 = 15$ km), and medium attenuation $a_0 = 3.33 \times 10^{-3}$ Np/km (i.e., $\alpha = 0.05$ per characteristic wavelength). Two sample durations are considered: $T = 100$ ks and $T = 500$ ks (approximately 27 h and 139 h) corresponding, respectively, to $\mathrm{N} = 4 \times 10^4$ and $\mathrm{N} = 2 \times 10^5$ independent samples at the chosen bandwidth.

Figure 2 presents a selection of realizations of the sample covariance at a combination of values of sensor separation and sample duration. Denoting the observed magnitude of the peak of the sample covariance and its corresponding lag as $\widetilde{C}_p$ and $\tilde{\tau}$, respectively, the sample SNR is defined $\widetilde{Q} \equiv \widetilde{C}_p/\tilde{\nu}$, where $\tilde{\nu}$ represents the observed root-mean-square amplitude of the fluctuations over the sample. As demonstrated in Fig. 2, the observed SNR (ensemble average of $\widetilde{Q}$) compares favorably with its

expectation, $\mathcal{Q}$, derived in Sec. 3.1. Note the increase of SNR with sample duration and its decrease with aperture.

From Sec. 3.1 the speed and attenuation parameter estimates for the PE are given by $\tilde{c} \equiv d/(\tilde{\tau} c_0)$ and $\tilde{a} \equiv (\alpha\mu)^{-1} \ln[(2\pi\sqrt{2\mu\tilde{C}_p})/(\tilde{\nu}\sqrt{\tilde{c}})]$, respectively. For the FE, the minimum mean square error of the objective function $\tilde{c} = \text{argmin}_c\{\Phi\}$ yields the speed parameter estimate (and similarly for the attenuation). For each parameter and estimation strategy the percent error of the ensemble, $\tilde{\delta} \equiv [\mathrm{M}^{-1}\sum_{m=1}^{\mathrm{M}} (\tilde{\mathcal{J}} - 1)^2]^{1/2} \times 100$ $(\tilde{\mathcal{J}} = \tilde{c}, \tilde{a})$, is presented in Fig. 2. As an example, the percent error of the ensemble of joint estimates for speed and attenuation are plotted along with the data ensemble error ellipse for the case $d = 150$ km $(\mu = 10)$ and $T = 100$ ks. For comparison, the predicted bound on the percent error, $\delta \equiv \mathcal{J}^{-1/2} \times 100$ $(\mathcal{J} = I_c^{\mathrm{PE}}, I_c^{\mathrm{FE}}, I_a^{\mathrm{PE}})$, is plotted along with each observed result in Fig. 2.

The favorable agreement between the observed inversion error and the calculated bounds suggests that the derived CRB expressions can be predictive for uncertainty. As expected, the observed error decreases with sample duration and exhibits a minimum at the predicted optimal value of sensor separation, $d_{\max} = \mu_{\max}\lambda_0 = \lambda_0/(2\alpha) = 150$ km. At the smallest separation considered, $d = 15$ km $(\mu = 1)$, the inversion error is quite large (i.e., information vanishes at small separation). The PE strategy fails below an SNR threshold value of about $\tilde{Q} \approx 5$ (when the peak coherent power approaches the power of the fluctuations). A failure in this regime is not expected nor observed with the FE. As there is more information in the phase than the amplitude of the measurement, the relative error of the attenuation estimates is significantly larger than that of the phase speed.

4. Conclusion

A general approach has been presented for quantifying the FI and corresponding CRBs for ambient noise correlation parameter estimates. As a demonstration, the FI was calculated for the canonical case of a pair of sensors in isotropic noise in a 2D attenuating free space medium. From this, the CRB for medium speed and attenuation were derived in terms of the measurement duration, bandwidth, and sensor separation. As a validation, the calculated bounds were shown to be predictive of the estimation error observed in an inversion applied to simulated data. Though the estimation error decreases monotonically with increasing duration, it does not vary monotonically with separation. Rather, the error exhibits a global minimum at a value that depends on the tradeoff between sensor aperture resolution and SNR.[19]

While the approach has been demonstrated for two sensors in an isotropic seismic scenario, it is easily adapted to multiple sensors for scenarios for which canonical models exist, for example, isotropic noise in the deep[20] and shallow[21] ocean, as well as directional scenarios in both seismics[22] and the ocean.[23] The approach can be useful for predicting and analyzing the potential of existing data to yield useful results (e.g., has enough data been collected to achieve a desired level of confidence?) as well as for optimizing experimental design (e.g., sensor placement and operating frequencies, etc.). Further, the technique can complement efforts, such as bootstrapping,[18] to assign confidence to experimental measures generated from a small number of observations.[24]

Acknowledgments

This research was supported by ONR, Ocean Acoustics Code 322.

References and links

[1]C. Eckart, "The theory of noise in continuous media," J. Acoust. Soc. Am. **25**, 195–199 (1953).
[2]S. Fried, W. Kuperman, K. Sabra, and P. Roux, "Extracting the local Green's function on a horizontal array from ambient ocean noise," J. Acoust. Soc. Am. **124**, EL183–EL188 (2008).

[3]K. Sabra, P. Gerstoft, P. Roux, W. Kuperman, and M. Fehler, "Extracting time-domain Green's function estimates from ambient seismic noise," Geophys. Res. Lett. **32**, L03310, doi:10.1029/2004GL021862 (2005).
[4]A. Baggeroer, W. Kuperman, and H. Schmidt, "Matched field processing: Source localization in correlated noise as an optimum parameter estimation problem," J. Acoust. Soc. Am. **83**, 571–587 (1988).
[5]A. Gatherer and T. Meng, "The Cramer-Rao bound for position and amplitude estimation of multiple pulses in Gaussian noise," IEEE Trans. Circuits Syst., II: Analog Digital Signal Process. **46**, 448–456 (1999).
[6]S. C. Walker, "A model for spatial coherence from directive ambient noise in attenuating, dispersive media," J. Acoust. Soc. Am. **132**, EL15–EL21 (2012).
[7]R. Snieder, "The theory of coda wave interferometry," Pure Appl. Geophys. **163**, 455–473 (2006).
[8]M. Siderius, H. Song, P. Gerstoft, W. S. Hodgkiss, P. Hursky, and C. Harrison, "Adaptive passive fathometer processing," J. Acoust. Soc. Am. **127**, 2193–2200 (2010).
[9]J. J. Freeman, "A systematic error in underwater acoustic direction-finding," J. Acoust. Soc. Am. **32**, 1025–1027 (1960).
[10]S. M. Kay, *Fundamentals of Statistical Signal Processing: Estimation Theory* (Prentice-Hall, Englewood Cliffs, NJ, 1993), Vol. 1, pp. 27–81.
[11]T. M. Cover and J. A. Thomas, *Elements of Information Theory*, 2nd ed. (Wiley-Interscience, New York, 2006), pp. 1–748.
[12]C. E. Shannon, "Communication in the presence of noise," Proc IEEE **72**, 1192–1201 (1984).
[13]N is alternately known as the degrees of freedom and the time-bandwidth product.
[14]The power spectrum for diffuse noise can depend on speed, attenuation, and frequency (Ref. 6). The white noise assumption implies a simplification that is consistent with experimental and theoretical efforts that neglect the information carried by the power spectra (Refs. 2, 3, and 22).
[15]From the central limit theorem $\nu_N = \nu/\sqrt{N} (N \gg 1)$.
[16]For physical systems, the covariance must have compact support over τ.
[17]M. W. Davis, "Production of conditional simulations via the LU triangular decomposition of the covariance matrix," Math. Geol. **19**, 91–98 (1987).
[18]J. F. Lawrence and G. A. Prieto, "Attenuation tomography of the western United States from ambient noise," J. Geophys. Res. **116**, 1–11, doi:10.1029/2010JB007836 (2011).
[19]This observation is not specific to 2D isotropic noise. The SNR/resolution tradeoff with separation leads to similar behavior of the error for a wide range of ambient noise scenarios.
[20]B. Cron and C. Sherman, "Spatial-correlation functions for various noise models," J. Acoust. Soc. Am. **34**, 1732–1736 (1961).
[21]W. Kuperman and F. Ingenito, "Spatial correlation of surface generated noise in a stratified ocean," J. Acoust. Soc. Am. **67**, 1988–1996 (1980).
[22]V. C. Tsai, "Understanding the amplitudes of noise correlation measurements," J. Geophys. Res. **116**, B09311, doi:10.1029/2011JB008483 (2011).
[23]S. C. Walker, "A model for the spatial coherence of arbitrarily directive noise in the depth-stratified ocean," J. Acoust. Soc. Am. **131**, EL388–EL394 (2012).
[24]M. Wall, J. Boen, and R. Tweedie, "An effective confidence interval for the mean with samples of size one and two," Am. Stat. **55**, 102–105 (2001).